

---

# Triple Generative Adversarial Nets

---

**Chongxuan Li**

Department of Computer Science  
Tsinghua University  
licx14@mails.tsinghua.edu.cn

**Kun Xu**

Department of Computer Science  
Tsinghua University  
xu-k16@mails.tsinghua.edu.cn

**Jun Zhu**

Department of Computer Science  
Tsinghua University  
dcszj@mail.tsinghua.edu.cn

**Bo Zhang**

Department of Computer Science  
Tsinghua University  
dcszb@mail.tsinghua.edu.cn

## Abstract

Generative Adversarial Nets (GANs) have shown promise in image generation and semi-supervised learning (SSL). However, existing GANs in SSL have two problems: (1) the generator and discriminator may compete in learning; and (2) the generator cannot generate images in a specific class. The problems essentially arise from the two-player formulation, where a single discriminator shares incompatible roles of identifying fake samples and predicting labels and it only estimates the data without considering labels. We address the problems by presenting triple generative adversarial net (Triple-GAN), a flexible game-theoretical framework for classification and class-conditional generation in SSL. Triple-GAN consists of three players—a generator, a discriminator and a classifier, where the generator and classifier characterize the conditional distributions between images and labels, and the discriminator solely focuses on identifying fake image-label pairs. We design compatible utilities to ensure that the distributions characterized by the classifier and generator both concentrate to the data distribution. Our results on various datasets demonstrate that Triple-GAN as a unified model can simultaneously (1) achieve state-of-the-art classification results among deep generative models, and (2) disentangle the classes and styles and transfer smoothly on the data level via interpolation in the latent space class-conditionally.

## 1 Introduction

Deep generative models (DGMs) can capture the underlying distributions of the data and synthesize new samples. Recently, significant progress has been made on generating realistic images based on Generative Adversarial Nets (GANs) [7, 3, 22]. GAN is formulated as a two-player game, where the generator  $G$  takes a random noise  $z$  as input and produces a sample  $G(z)$  in the data space while the discriminator  $D$  identifies whether a certain sample comes from the true data distribution  $p(x)$  or the generator. Both  $G$  and  $D$  are parameterized as deep neural networks and the training procedure is to solve a minimax problem:

$$\min_G \max_D U(D, G) = E_{x \sim p(x)} [\log(D(x))] + E_{z \sim p_z(z)} [\log(1 - D(G(z)))],$$

where  $p_z(z)$  is a simple distribution (e.g., uniform or normal) and  $U(\cdot)$  denotes the utilities. Given a generator and the defined distribution  $p_g$ , the optimal discriminator is  $D(x) = p(x)/(p_g(x) + p(x))$  under the assumption of infinite capacity, and the global equilibrium of this game achieves if and only if  $p_g(x) = p(x)$  [7], which is desired in terms of image generation.

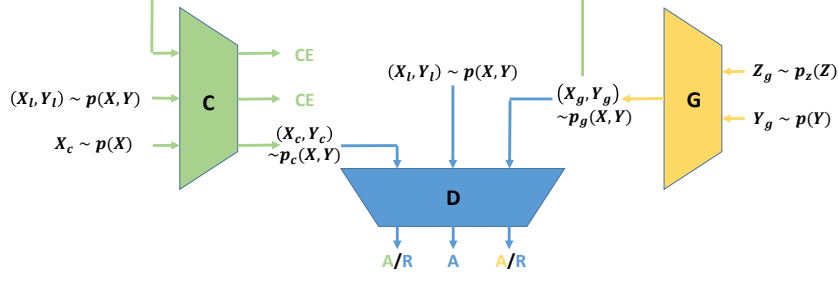


Figure 1: An illustration of Triple-GAN (best view in color). The utilities of  $D$ ,  $C$  and  $G$  are colored in blue, green and yellow respectively, with “R” denoting rejection, “A” denoting acceptance and “CE” denoting the cross entropy loss for supervised learning. “A”s and “R”s are the adversarial losses and “CE”s are unbiased regularizations that ensure the consistency between  $p_g$ ,  $p_c$  and  $p$ .

GANs and DGMs in general have also proven effective in semi-supervised learning (SSL) [11], while retaining the generative capability. Under the same two-player game framework, Cat-GAN [26] generalizes GANs with a categorical discriminative network and an objective function that minimizes the conditional entropy of predictions given data while maximizes the conditional entropy of predictions given generated samples. Odena [20] and Salimans et al. [25] augment the categorical discriminator with one more class, corresponding to the fake data generated by the generator. There are two main problems in existing GANs for SSL: (1) the generator and discriminator (i.e., classifier) may compete in learning; and (2) the generator cannot generate images in a specific class.

For the first problem, as an instance, Salimans et al. [25] propose two alternative training objectives that work well for either classification or image generation in SSL, but not both. The objective of *feature matching* works well in classification but fails to generate indistinguishable samples (See Sec.5.2 for examples), while the other objective of *minibatch discrimination* is good at realistic image generation but cannot predict labels accurately. The competition between  $G$  and  $D$  essentially arises from their two-player formulation, where a single discriminator network has to play two incompatible roles—identifying fake samples and predicting labels. Such a shared architecture can prevent the model from achieving a desirable equilibrium. Specifically, if  $G$  is optimal, namely  $p(x) = p_g(x)$ , then given a sample  $x \sim p_g(x)$ , as a discriminator,  $D$  should identify it as fake data with non-zero probability (See [7] for proof). However, as a classifier, the optimal  $D$  should always predict the correct class of  $x$  confidently since  $x \sim p(x)$ . It conflicts as  $D$  has two incompatible converge points, which indicates that either  $G$  or  $D$  won’t achieve its own optimum. Namely, the learning capacity of existing models is restricted, which should be addressed to advance current SSL results.

For the second problem, existing GANs in SSL [26, 25] cannot generate data given certain class because the discriminator focuses on estimating the marginal distribution of data without considering labels and the generator cannot leverage the missing labels inferred by the discriminator. However, disentangling meaningful physical factors like object category from latent representations with limited supervision is of general interest [30, 2]. To our best knowledge, no existing GAN-based model generates data class-conditionally in SSL, though some [22, 5, 21] can do this given full labels.

We address these issues by presenting Triple-GAN, a flexible game-theoretical framework for both classification and class-conditional image generation in SSL, where the data is characterized by a joint distribution  $p(x, y)$  of input  $x$  and label  $y$ . Based on the alternative factorizations  $p(x, y) = p(y)p(x|y)$  and  $p(x, y) = p(x)p(y|x)$ , we build two separate conditional models—a generator and a classifier, to characterize the conditional distributions  $p(x|y)$  and  $p(y|x)$ , respectively. By mildly assuming that samples can be drawn from the marginal distributions  $p(x)$  and  $p(y)$ , we can draw input-label pairs  $(x, y)$  from  $p_g(x, y)$  and  $p_c(x, y)$ , the distributions defined by our generator and classifier. Then, we define an adversarial game (See Fig. 1 for its illustration) by introducing a discriminator which has the single role of determining whether a sample  $(x, y)$  is from the model distribution or the data distribution. Directly motivated by the desirable equilibrium that both  $p_g$  and  $p_c$  concentrate to the true data distribution  $p$ , we carefully design compatible utilities including adversarial losses and unbiased regularizations, which leads to an effective solution to the challenging SSL task. Specifically, in Triple-GAN, instead of competing as stated in the first problem, a good classifier will result in a good generator via teaching the shared discriminator and vice versa. Furthermore, the generator can leverage the missing labels inferred by the classifier implicitly through the discriminator and hence the generator can be trained class-conditionally, which addresses the second problem.

We evaluate our model on the widely adopted MNIST [14], SVHN [19] and CIFAR10 [12] datasets. The results (See Sec. 5) demonstrate that Triple-GAN can simultaneously learn a good classifier and a conditional generator, which agrees with our motivation and theoretical results (See Sec. 3.2).

Overall, our main contributions are two folded: (1) we analyze the problems in existing SSL GANs [26, 25] and propose a novel game-theoretical Triple-GAN framework to address them with carefully designed compatible objectives; and (2) we show that on the three datasets with incomplete labels, Triple-GAN can advance the state-of-the-art classification results of DGMs substantially and, at the same time, disentangle classes and styles and perform class-conditional interpolation.

## 2 Related Work

Various approaches have been developed to learn DGMs, including MLE-based models such as Variational Autoencoders (VAEs) [10, 24], Generative Moment Matching Networks (GMMNs) [16, 6] and Generative Adversarial Nets (GANs) [7]. These criteria are systematically compared in [28].

One primal goal of DGMs is to generate realistic samples, for which GANs have proven effective. Specifically, LAP-GAN [3] leverages a series of GANs to upscale the generated samples to high resolution images through the Laplacian pyramid framework [1]. DCGAN [22] adopts (fractionally) strided convolution layers and batch normalization [8] in GANs and generates realistic natural images.

Recent work has introduced inference networks in GANs. For instance, InfoGAN [2] learns interpretable latent codes from unlabeled data by regularizing the original GANs via variational mutual information maximization. In ALI [5, 4], the inference network approximates the posterior distribution of latent variables given true data in unsupervised manner. Triple-GAN also has an inference network (classifier) as in ALI but there exist two important differences in global equilibria and utilities between them: (1) Triple-GAN matches both the distributions defined by the generator and classifier to true data distribution while ALI only ensures that the distributions defined by the generator and inference network to be the same; (2) the discriminator will reject the samples from the classifier in Triple-GAN while the discriminator will accept the samples from the inference network in ALI, which leads to different update rules for the discriminator and inference network. These differences naturally arise because Triple-GAN is proposed to solve the existing problems in SSL GANs as stated in the introduction. Indeed, ALI [5] uses the same approach as [25] to deal with partially labeled data and hence it still suffers from the problems. In addition, Triple-GAN outperforms ALI significantly in terms of semi-supervised classification (See comparison in Table. 1).

To handle partially labeled data, the conditional VAE [11] treats the missing labels as latent variables and infer them for unlabeled data. ADGM [17] introduces auxiliary variables to build a more expressive variational distribution and improve the predictive performance. The Ladder Network [23] employs lateral connections between a variation of denoising autoencoders and obtains excellent SSL results. Cat-GAN [26] generalizes GANs with a categorical discriminative network and an objective function. Salimans et al. [25] propose empirical techniques to stabilize the training of GANs and improve the performance on SSL and image generation under incompatible learning criteria. Triple-GAN differs significantly from these methods, as stated in the introduction.

## 3 Method

We consider learning DGMs in the semi-supervised setting,<sup>1</sup> where we have a partially labeled dataset with  $x$  denoting input and  $y$  denoting the output label. The goal is to predict the labels  $y$  for unlabeled data as well as to generate new samples  $x$  conditioned on  $y$ . This is different from the unsupervised setting for pure generation, where the only goal is to sample data  $x$  from a generator to fool a discriminator; thus a two-player game is sufficient to describe the process as in GANs. In our setting, as the label information  $y$  is incomplete (thus uncertain), our density model should characterize the uncertainty of both  $x$  and  $y$ , therefore a joint distribution  $p(x, y)$  of input-label pairs.

A straightforward application of the two-player GAN is infeasible because of the missing values on  $y$ . Unlike the previous work [26, 25], which is restricted to the two-player framework and can lead to incompatible objectives, we build our game-theoretic objective based on the insight that the joint distribution can be factorized in two ways, namely,  $p(x, y) = p(x)p(y|x)$  and  $p(x, y) = p(y)p(x|y)$ ,

<sup>1</sup>Supervised learning is an extreme case, where the training set is fully labeled.

and that the conditional distributions  $p(y|x)$  and  $p(x|y)$  are of interest for classification and class-conditional generation, respectively. To jointly estimate these conditional distributions, which are characterized by a classifier network and a class-conditional generator network, we define a single discriminator network which has the sole role of distinguishing whether a sample is from the true data distribution or the models. Hence, we naturally extend GANs to Triple-GAN, a three-player game to characterize the process of classification and class-conditional generation in SSL, as detailed below.

### 3.1 A Game with Three Players

Triple-GAN consists of three components: (1) a classifier  $C$  that (approximately) characterizes the conditional distribution  $p_c(y|x) \approx p(y|x)$ ; (2) a class-conditional generator  $G$  that (approximately) characterizes the conditional distribution in the other direction  $p_g(x|y) \approx p(x|y)$ ; and (3) a discriminator  $D$  that distinguishes whether a pair of data  $(x, y)$  comes from the true distribution  $p(x, y)$ . All the components are parameterized as neural networks. Our desired equilibrium is that the joint distributions defined by the classifier and generator will concentrate to the true data distribution. To this end, we design a game with compatible utilities for triple players as follows.

We make the mild assumption that the samples from both  $p(x)$  and  $p(y)$  can be easily obtained.<sup>2</sup> In the game, after a sample  $x$  is drawn from  $p(x)$ ,  $C$  produces a pseudo label  $y$  given  $x$  following the conditional distribution  $p_c(y|x)$ . Hence, the pseudo input-label pair is a sample from the joint distribution  $p_c(x, y) = p(x)p_c(y|x)$ . Similarly, a pseudo input-label pair can be sampled from  $G$  by first drawing  $y \sim p(y)$  and then drawing  $x|y \sim p_g(x|y)$ ; hence from the joint distribution  $p_g(x, y) = p(y)p_g(x|y)$ . For  $p_g(x|y)$ , we assume that  $x$  is transformed by the latent style variables  $z$  given the label  $y$ , namely,  $x = G(y, z)$ ,  $z \sim p_z(z)$ , where  $p_z(z)$  is a simple distribution (e.g., uniform or standard normal). Then, the pseudo input-label pairs  $(x, y)$  generated by both  $C$  and  $G$  are sent to the single discriminator  $D$  for judgement.  $D$  can also access the input-label pairs from the true data distribution as positive samples. We refer the utilities in the process as adversarial losses, which can be formulated as a minimax game:

$$\min_{C, G} \max_D U(C, G, D) = E_{(x, y) \sim p(x, y)} [\log D(x, y)] \\ + (1 - \alpha) E_{y \sim p(y), z \sim p_z(z)} [\log(1 - D(G(y, z), y))] + \alpha E_{x \sim p(x), y \sim p_c(y|x)} [\log(1 - D(x, y))], \quad (1)$$

where  $\alpha \in (0, 1)$  is a constant that controls the relative importance of generation and classification and we focus on the balance case by fixing it as  $1/2$  throughout the paper.

The game defined in Eqn. (1) achieves the equilibrium if and only if  $p(x, y) = (1 - \alpha)p_g(x, y) + \alpha p_c(x, y)$  (See details in Sec. 3.2). The equilibrium indicates that if one of  $C$  and  $G$  tends to the data distribution, the other will also go towards the data distribution, which addresses the competing problem. However, unfortunately, it cannot guarantee that  $p(x, y) = p_g(x, y) = p_c(x, y)$  is the unique global optimum, which is not desirable. To address this problem, we introduce the standard supervised loss (i.e., cross-entropy loss) to  $C$ ,  $\mathcal{R}_{\mathcal{L}} = E_{(x, y) \sim p(x, y)} [-\log p_c(y|x)]$ , which is equivalent to the KL-divergence between  $p_c(x, y)$  and  $p(x, y)$ . Consequently, we define the game as:

$$\min_{C, G} \max_D \tilde{U}(C, G, D) = E_{(x, y) \sim p(x, y)} [\log D(x, y)] + \mathcal{R}_{\mathcal{L}} \\ + (1 - \alpha) E_{y \sim p(y), z \sim p_z(z)} [\log(1 - D(G(y, z), y))] + \alpha E_{x \sim p(x), y \sim p_c(y|x)} [\log(1 - D(x, y))]. \quad (2)$$

It will be proven that the game with utilities  $\tilde{U}$  has the unique global optimum for  $C$  and  $G$ .

### 3.2 Theoretical Analysis and Pseudo Discriminative Loss

We now provide a formal theoretical analysis of Triple-GAN under nonparametric assumptions and introduce pseudo discriminative loss, which is an unbiased regularization motivated by the global equilibrium. For clarity of the main text, we defer the proof details to Appendix A.

First, we can show that the optimal  $D$  balances between the true data distribution and the mixture distribution defined by  $C$  and  $G$ , as summarized in Lemma 3.1.

<sup>2</sup>In semi-supervised learning,  $p(x)$  is the empirical distribution of inputs and  $p(y)$  is assumed same to the distribution of labels on labeled data, which is uniform in our experiment.

---

**Algorithm 1** Minibatch stochastic gradient descent training of Triple-GAN in SSL.

---

**for** number of training iterations **do**

- Sample a batch of pairs  $(x_g, y_g) \sim p_g(x, y)$  of size  $m_g$ , a batch of pairs  $(x_c, y_c) \sim p_c(x, y)$  of size  $m_c$  and a batch of labeled data  $(x_d, y_d) \sim p(x, y)$  of size  $m_d$ .
- Update  $D$  by ascending along its stochastic gradient:

$$\nabla_{\theta_d} \left[ \frac{1}{m_d} \left( \sum_{(x_d, y_d)} \log D(x_d, y_d) \right) + \frac{\alpha}{m_c} \sum_{(x_c, y_c)} \log(1 - D(x_c, y_c)) + \frac{1 - \alpha}{m_g} \sum_{(x_g, y_g)} \log(1 - D(x_g, y_g)) \right].$$

- Compute the unbiased estimators  $\tilde{\mathcal{R}}_{\mathcal{L}}$  and  $\tilde{\mathcal{R}}_{\mathcal{P}}$  of  $\mathcal{R}_{\mathcal{L}}$  and  $\mathcal{R}_{\mathcal{P}}$  respectively.
- Update  $C$  by descending along its stochastic gradient:

$$\nabla_{\theta_c} \left[ \frac{\alpha}{m_c} \sum_{(x_c, y_c)} p_c(y_c | x_c) \log(1 - D(x_c, y_c)) + \tilde{\mathcal{R}}_{\mathcal{L}} + \alpha_{\mathcal{P}} \tilde{\mathcal{R}}_{\mathcal{P}} \right].$$

- Update  $G$  by descending along its stochastic gradient:

$$\nabla_{\theta_g} \left[ \frac{1 - \alpha}{m_g} \sum_{(x_g, y_g)} \log(1 - D(x_g, y_g)) \right].$$

**end for**

---

**Lemma 3.1.** *For any fixed  $C$  and  $G$ , the optimal  $D$  of the game defined by the utility function  $U(C, G, D)$  is:*

$$D_{C,G}^*(x, y) = \frac{p(x, y)}{p(x, y) + p_{\alpha}(x, y)}, \quad (3)$$

where  $p_{\alpha}(x, y) := (1 - \alpha)p_g(x, y) + \alpha p_c(x, y)$  is a valid distribution.

Given  $D_{C,G}^*$ , we can omit  $D$  and reformulate the minimax game with value function  $U$  as:  $V(C, G) = \max_D U(C, G, D)$ , whose optimal point is summarized as in Lemma 3.2.

**Lemma 3.2.** *The global minimum of  $V(C, G)$  is achieved if and only if  $p(x, y) = p_{\alpha}(x, y)$ .*

We can further show that  $C$  and  $G$  can at least capture the marginal distribution of data, especially for  $p_g(x)$ , even there may exist multiple global equilibria, as summarized in Corollary 3.2.1.

**Corollary 3.2.1.** *Given  $p(x, y) = p_{\alpha}(x, y)$ , the marginal distributions are the same for  $p$ ,  $p_c$  and  $p_g$ .*

Given the above result that  $p(x, y) = p_{\alpha}(x, y)$ ,  $C$  and  $G$  do not compete as in the two-player based formulation and it is easy to verify that  $p(x, y) = p_c(x, y) = p_g(x, y)$  is a global equilibrium point. However, it may not be unique and we should minimize an additional objective to ensure the uniqueness. In fact, this is true for the utility function  $\tilde{U}(C, G, D)$  in problem (2), as stated below.

**Theorem 3.3.** *The equilibrium of  $\tilde{U}(C, G, D)$  is achieved if and only if  $p(x, y) = p_g(x, y) = p_c(x, y)$ .*

The conclusion essentially motivates our design of Triple-GAN, as we can ensure that both  $C$  and  $G$  will concentrate to the true data distribution if the model has been trained to achieve the optimum.

We can further show another nice property of  $\tilde{U}$ , which allows us to regularize our model for stable and better convergence in practice without bias, as summarized below.

**Corollary 3.3.1.** *Any additional regularization on the distances between the marginal, conditional and joint distributions of any two players, will not change the global equilibrium of  $\tilde{U}$ .*

Because label information is extremely insufficient in SSL, we propose *pseudo discriminative loss*  $\mathcal{R}_{\mathcal{P}} = E_{p_g}[-\log p_c(y|x)]$ , which optimizes  $C$  on the samples generated by  $G$  in supervised manner. Intuitively, a good  $G$  can provide meaningful labeled data beyond the training set as extra side information for  $C$ , which will boost the predictive performance (See Sec. 5.1 for empirical evidence). Indeed, minimizing pseudo discriminative loss with respect to  $C$  is equivalent to minimizing  $D_{KL}(p_g(x, y) || p_c(x, y))$  (See Appendix A for proof) and hence the global equilibria remains following Corollary 3.3.1. Note that directly minimizing  $D_{KL}(p_g(x, y) || p_c(x, y))$  is infeasible since its computation involves the unknown likelihood ratio  $p_g(x, y)/p_c(x, y)$ . The pseudo discriminative

loss is weighted by a hyperparameter  $\alpha_{\mathcal{P}}$ . See Algorithm 1 for the whole training procedure, where  $\theta_c$ ,  $\theta_d$  and  $\theta_g$  are trainable parameters in  $C$ ,  $D$  and  $G$  respectively.

## 4 Practical Techniques

In this section we introduce several practical techniques used in the implementation of Triple-GAN, which may lead to a biased solution theoretically but work well for challenging SSL tasks empirically.

One crucial problem of SSL is the small size of labeled data. In Triple-GAN,  $D$  may memorize the empirical distribution of labeled data, and reject other types of samples from the true data distribution. Consequently,  $G$  may collapse to these modes. To avoid this, we generate pseudo labels through  $C$  for some unlabeled data and use these pairs as positive samples of  $D$ . The cost is on introducing some bias to the target distribution of  $D$ , which is a mixture of  $p_c$  and  $p$  instead of pure  $p$ . But this is acceptable as  $C$  converges quickly and  $p_c$  and  $p$  are close (See results in Sec.5).

Since properly leveraging unlabeled data is key to success in SSL, it is necessary to regularize  $C$  heuristically as in many existing methods [23, 26, 13, 15] to make more accurate predictions. We consider two alternative losses on the unlabeled data. Confidence loss [26] minimizes the conditional entropy of  $p_c(y|x)$  and the cross entropy between  $p(y)$  and  $p_c(y)$ , weighted by a hyperparameter  $\alpha_{\mathcal{B}}$ , as  $\mathcal{R}_{\mathcal{U}} = H_{p_c}(y|x) + \alpha_{\mathcal{B}} E_p[-\log p_c(y)]$ , which encourages  $C$  to make predictions confidently and be balanced on unlabeled data. Consistency loss [13] penalizes the network if it predicts the same unlabeled data inconsistently given different noise  $\epsilon$ , e.g., dropout masks, as  $\mathcal{R}_{\mathcal{U}} = E_{x \sim p(x)} \|p_c(y|x, \epsilon) - p_c(y|x, \epsilon')\|^2$ , where  $\|\cdot\|^2$  is the square of the  $l_2$ -norm. We use the confidence loss by default except on the CIFAR10 dataset (See details in Sec. 5).

Another consideration is to compute the gradients of  $E_{x \sim p(x), y \sim p_c(y|x)} [\log(1 - D(x, y))]$  with respect to the parameters  $\theta_c$  in  $C$ , which involves summation over the discrete random variable  $y$ . Because directly integrating out  $y$  is time-consuming, we use a variant of the REINFORCE algorithm [29], in which the gradients should be  $E_{x \sim p(x)} E_{y \sim p_c(y|x)} [\nabla_{\theta_c} \log p_c(y|x) \log(1 - D(x, y))]$ . In our experiment, we find the best strategy is to use most probable  $y$  instead of sampling one to approximate the expectation over  $y$ . The bias is small as the prediction of  $C$  is rather confident typically.

## 5 Experiments

We now present results on the widely adopted MNIST [14], SVHN [19], and CIFAR10 [12] datasets. MNIST consists of 50,000 training samples, 10,000 validation samples and 10,000 testing samples of handwritten digits of size  $28 \times 28$ . SVHN consists of 73,257 training samples and 26,032 testing samples and each is a colored image of size  $32 \times 32$ , containing a sequence of digits with various backgrounds. CIFAR10 consists of colored images distributed across 10 general classes—*airplane*, *automobile*, *bird*, *cat*, *deer*, *dog*, *frog*, *horse*, *ship* and *truck*. There are 50,000 training samples and 10,000 samples of size  $32 \times 32$  in CIFAR10. We split 5,000 training data of SVHN and CIFAR10 for validation if needed. On CIFAR10, we follow [13] to perform ZCA for the input of  $C$  but still generate and estimate the raw images using  $G$  and  $D$ .

We implement our method on Theano [27] and here we briefly summarize our experimental settings.<sup>3</sup> For fair comparison, we follow [26, 25] to split the training dataset (Results are averaged over 10 random splits of data) and choose architectures (See details in Appendix F). We do not tune the hyperparameters heavily. The pseudo discriminative loss is not applied until the number of epochs reach a threshold that the generator could generate meaningful data. We only search the threshold in  $\{200, 300\}$ ,  $\alpha_{\mathcal{P}}$  in  $\{0.1, 0.03\}$  and the global learning rate in  $\{0.0003, 0.001\}$  based on the validation performance on each dataset. All of the other hyperparameters including relative weights and parameters in Adam [9] are fixed according to [25, 15] across all of the experiments. Further, in our experiments, we find that the training techniques for the original two-player GANs [3, 25] are sufficient to stabilize the optimization of Triple-GAN.

### 5.1 Classification

Firstly, we compare our method with a large body of approaches in the widely used settings on MNIST, SVHN and CIFAR10 datasets given 100, 1,000 and 4,000 labels respectively. Table 1 summarizes the quantitative results. On all of the three datasets, Triple-GAN achieves state-of-the-art results consistently and it substantially outperforms the strongest competitors (e.g., ALI and Improved-GAN)

<sup>3</sup>Our source code is available at <https://github.com/zhenxuan00/triple-gan>.

Table 1: Error rates (%) on partially labeled MNIST, SVHN and CIFAR10 datasets. The results with <sup>†</sup> are trained with more than 500,000 extra unlabeled data on SVHN.

Algorithm	MNIST $n = 100$	SVHN $n = 1000$	CIFAR10 $n = 4000$
<i>M1+M2</i> [11]	3.33 ( $\pm 0.14$ )	36.02 ( $\pm 0.10$ )	
<i>VAT</i> [18]	2.33		24.63
<i>Ladder</i> [23]	1.06 ( $\pm 0.37$ )		20.40 ( $\pm 0.47$ )
<i>Conv-Ladder</i> [23]	<b>0.89</b> ( $\pm 0.50$ )		
<i>ADGM</i> [17]	0.96 ( $\pm 0.02$ )	22.86 <sup>†</sup>	
<i>SDGM</i> [17]	1.32 ( $\pm 0.07$ )	16.61 ( $\pm 0.24$ ) <sup>†</sup>	
<i>MMCVA</i> [15]	1.24 ( $\pm 0.54$ )	<b>4.95</b> ( $\pm 0.18$ ) <sup>†</sup>	
<i>CatGAN</i> [26]	1.39 ( $\pm 0.28$ )		19.58 ( $\pm 0.58$ )
<i>Improved-GAN</i> [25]	0.93 ( $\pm 0.07$ )	8.11 ( $\pm 1.3$ )	18.63 ( $\pm 2.32$ )
<i>ALI</i> [5]		7.3	18.3
<i>Triple-GAN (ours)</i>	<b>0.91</b> ( $\pm 0.58$ )	<b>5.77</b> ( $\pm 0.17$ )	<b>16.99</b> ( $\pm 0.36$ )

Table 2: Error rates (%) on MNIST with different number of labels.

Algorithm	$n = 20$	$n = 50$	$n = 200$
<i>Improved-GAN</i> [25]	16.77 ( $\pm 4.52$ )	2.21 ( $\pm 1.36$ )	0.90 ( $\pm 0.04$ )
<i>Triple-GAN (ours)</i>	<b>4.81</b> ( $\pm 4.95$ )	<b>1.56</b> ( $\pm 0.72$ )	<b>0.67</b> ( $\pm 0.16$ )

on more challenging SVHN and CIFAR10 datasets, which demonstrate the benefit of compatible learning objectives proposed in Triple-GAN. Note that for a fair comparison with previous GANs, we do not leverage the extra unlabeled data on SVHN, while some baselines [17, 15] do.

Secondly, we evaluate our method with 20, 50 and 200 labeled samples on MNIST for a systematical comparison with our main baseline Improved-GAN [25], as shown in Table 2. Triple-GAN consistently outperforms Improved-GAN with a substantial margin, which again demonstrates the benefit of Triple-GAN. Besides, we can see that Triple-GAN achieves more significant improvement as the number of labeled data decreases, suggesting the effectiveness of the pseudo discriminative loss.

Finally, we investigate the reasons for the outstanding performance of Triple-GAN. We train a single  $C$  without  $G$  and  $D$  on SVHN as the baseline and get more than 10% error rate, which shows that  $G$  is important for SSL even though  $C$  can leverage unlabeled data directly. On CIFAR10, the baseline (a simple version of  $\Pi$  model [13]) achieves 17.7% error rate. The smaller improvement is reasonable as CIFAR10 is more complex and hence  $G$  is not as good as in SVHN. In addition, we evaluate Triple-GAN without the pseudo discriminative loss on SVHN and it achieves about 7.8% error rate, which shows the advantages of compatible objectives (better than the 8.11% error rate of Improved-GAN) and the importance of the pseudo discriminative loss (worse than the complete Triple-GAN by 2%). Furthermore, Triple-GAN has a comparable convergence speed with Improved-GAN [25], as shown in Appendix E.

## 5.2 Generation

We demonstrate that Triple-GAN can learn good  $G$  and  $C$  simultaneously by generating samples in various ways with the exact models used in Sec. 5.1. For fair comparison, the generative model and the number of labels are the same to the previous method [25].

In Fig. 2 (a-b), we first compare the quality of images generated by Triple-GAN on SVHN and the Improved-GAN with feature matching [25],<sup>4</sup> which works well for semi-supervised classification. We can see that Triple-GAN outperforms the baseline by generating fewer meaningless samples and clearer digits. Further, the baseline repeats to generate strange samples labeled with red rectangles in Fig. 2 but Triple-GAN does not. The comparison on MNIST and CIFAR10 is presented in Appendix B. We also evaluate the samples on CIFAR10 quantitatively via inception score following [25]. The value of Triple-GAN is  $5.08 \pm 0.09$  while that of the Improved-GAN trained without minibatch discrimination [25] is  $3.87 \pm 0.03$ , which agrees with the visual comparison. We then illustrate

<sup>4</sup>Though the Improved-GAN trained with minibatch discrimination [25] can generate good samples, it fails to predict labels accurately.



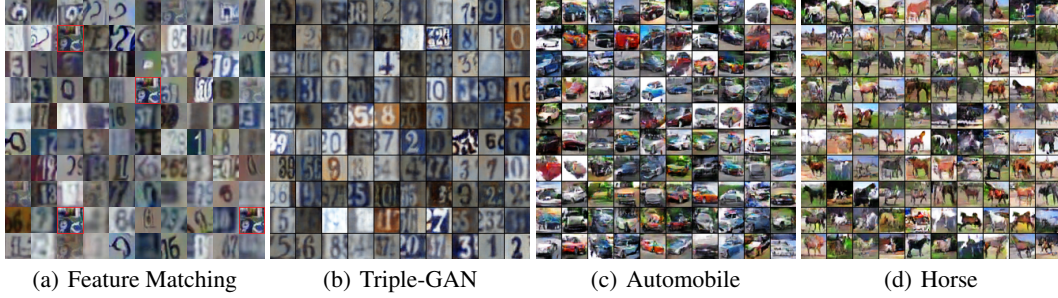


Figure 2: (a-b) Comparison between samples from Improved-GAN trained with feature matching and Triple-GAN on SVHN. (c-d) Samples of Triple-GAN in specific classes on CIFAR10.

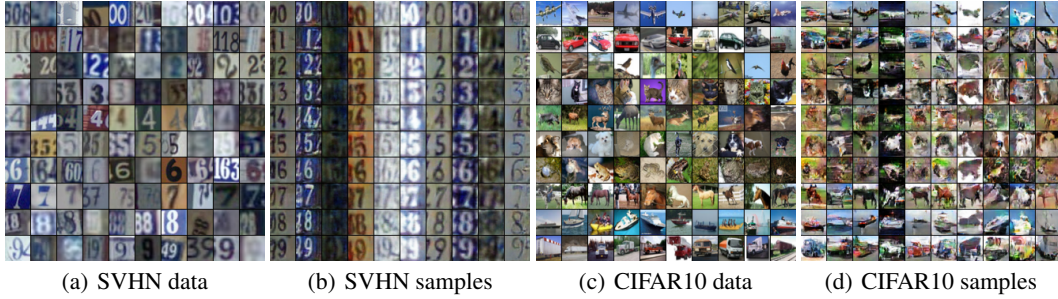


Figure 3: (a) and (c) are randomly selected labeled data. (b) and (d) are samples from Triple-GAN, where each row shares the same label and each column shares the same latent variables.

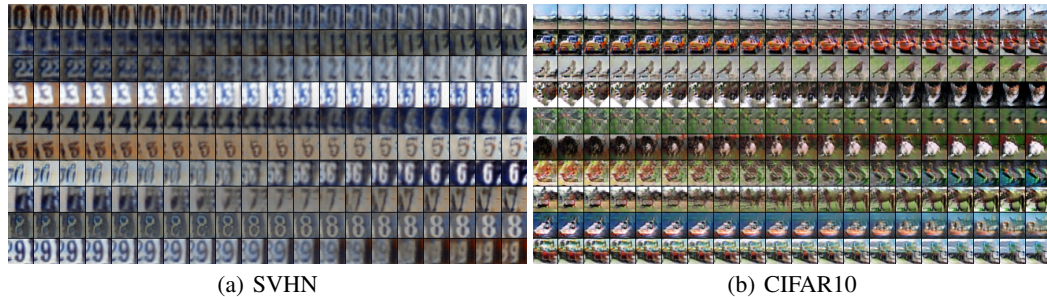


Figure 4: Class-conditional latent space interpolation. We first sample two random vectors in the latent space and interpolate linearly from one to another. Then, we map these vectors to the data level given a fixed label for each class. Totally, 20 images are shown for each class. We select two endpoints with clear semantics on CIFAR10 for better illustration.

images generated from two specific classes on CIFAR10 in Fig. 2 (c-d) and see more in Appendix C. In most cases, Triple-GAN is able to generate meaningful images with correct semantics.

Further, we show the ability of Triple-GAN to disentangle classes and styles in Fig. 3. It can be seen that Triple-GAN can generate realistic data in a specific class and the latent factors encode meaningful physical factors like: scale, intensity, orientation, color and so on. Some GANs [22, 5, 21] can generate data class-conditionally given full labels, while Triple-GAN can do similar thing given much less label information.

Finally, we demonstrate the generalization capability of our Triple-GAN on class-conditional latent space interpolation as in Fig. 4. Triple-GAN can transit smoothly from one sample to another with totally different visual factors without losing label semantics, which proves that Triple-GANs can learn meaningful latent spaces class-conditionally instead of overfitting to the training data, especially labeled data. See these results on MNIST in Appendix D.

Overall, these results confirm that Triple-GAN avoid the competition between  $C$  and  $G$  and can lead to a situation where both the generation and classification are good in semi-supervised learning.



## 6 Conclusions

We present triple generative adversarial networks (Triple-GAN), a unified game-theoretical framework with three players—a generator, a discriminator and a classifier, to do semi-supervised learning with compatible utilities, i.e., adversarial losses and unbiased regularizations. With such utilities, Triple-GAN addresses two main problems of existing methods [26, 25]. Specifically, Triple-GAN ensures that both the classifier and the generator can achieve its own optimum in the perspective of game theory and enable the generator to sample data in a specific class. Our empirical results on MNIST, SVHN and CIFAR10 datasets demonstrate that as a unified model, Triple-GAN can simultaneously achieve state-of-the-art classification results among deep generative models and disentangle styles and classes and transfer smoothly on the data level via interpolation in the latent space.

## References

- [1] Peter Burt and Edward Adelson. The Laplacian pyramid as a compact image code. *IEEE Transactions on communications*, 1983.
- [2] Xi Chen, Yan Duan, Rein Houthoofd, John Schulman, Ilya Sutskever, and Pieter Abbeel. InfoGAN: Interpretable representation learning by information maximizing generative adversarial nets. In *NIPS*, 2016.
- [3] Emily L Denton, Soumith Chintala, and Rob Fergus. Deep generative image models using a Laplacian pyramid of adversarial networks. In *NIPS*, 2015.
- [4] Jeff Donahue, Philipp Krähenbühl, and Trevor Darrell. Adversarial feature learning. *arXiv preprint arXiv:1605.09782*, 2016.
- [5] Vincent Dumoulin, Ishmael Belghazi, Ben Poole, Alex Lamb, Martin Arjovsky, Olivier Mastropietro, and Aaron Courville. Adversarially learned inference. *arXiv preprint arXiv:1606.00704*, 2016.
- [6] Gintare Karolina Dziugaite, Daniel M Roy, and Zoubin Ghahramani. Training generative neural networks via maximum mean discrepancy optimization. *arXiv preprint arXiv:1505.03906*, 2015.
- [7] Ian Goodfellow, Jean Pouget-Abadie, Mehdi Mirza, Bing Xu, David Warde-Farley, Sherjil Ozair, Aaron Courville, and Yoshua Bengio. Generative adversarial nets. In *NIPS*, 2014.
- [8] Sergey Ioffe and Christian Szegedy. Batch normalization: Accelerating deep network training by reducing internal covariate shift. *arXiv preprint arXiv:1502.03167*, 2015.
- [9] Diederik Kingma and Jimmy Ba. Adam: A method for stochastic optimization. *arXiv preprint arXiv:1412.6980*, 2014.
- [10] Diederik P Kingma and Max Welling. Auto-encoding variational Bayes. *arXiv preprint arXiv:1312.6114*, 2013.
- [11] Diederik P Kingma, Shakir Mohamed, Danilo Jimenez Rezende, and Max Welling. Semi-supervised learning with deep generative models. In *NIPS*, 2014.
- [12] Alex Krizhevsky and Geoffrey Hinton. Learning multiple layers of features from tiny images. *Citeseer*, 2009.
- [13] Samuli Laine and Timo Aila. Temporal ensembling for semi-supervised learning. *arXiv preprint arXiv:1610.02242*, 2016.
- [14] Yann LeCun, Léon Bottou, Yoshua Bengio, and Patrick Haffner. Gradient-based learning applied to document recognition. *Proceedings of the IEEE*, 86(11):2278–2324, 1998.
- [15] Chongxuan Li, Jun Zhu, and Bo Zhang. Max-margin deep generative models for (semi-) supervised learning. *arXiv preprint arXiv:1611.07119*, 2016.
- [16] Yujia Li, Kevin Swersky, and Richard S Zemel. Generative moment matching networks. In *ICML*, 2015.

- [17] Lars Maaløe, Casper Kaae Sønderby, Søren Kaae Sønderby, and Ole Winther. Auxiliary deep generative models. *arXiv preprint arXiv:1602.05473*, 2016.
- [18] Takeru Miyato, Shin-ichi Maeda, Masanori Koyama, Ken Nakae, and Shin Ishii. Distributional smoothing with virtual adversarial training. *arXiv preprint arXiv:1507.00677*, 2015.
- [19] Yuval Netzer, Tao Wang, Adam Coates, Alessandro Bissacco, Bo Wu, and Andrew Y Ng. Reading digits in natural images with unsupervised feature learning. In *NIPS workshop on deep learning and unsupervised feature learning*, 2011.
- [20] Augustus Odena. Semi-supervised learning with generative adversarial networks. *arXiv preprint arXiv:1606.01583*, 2016.
- [21] Augustus Odena, Christopher Olah, and Jonathon Shlens. Conditional image synthesis with auxiliary classifier gans. *arXiv preprint arXiv:1610.09585*, 2016.
- [22] Alec Radford, Luke Metz, and Soumith Chintala. Unsupervised representation learning with deep convolutional generative adversarial networks. *arXiv preprint arXiv:1511.06434*, 2015.
- [23] Antti Rasmus, Mathias Berglund, Mikko Honkela, Harri Valpola, and Tapani Raiko. Semi-supervised learning with ladder networks. In *NIPS*, 2015.
- [24] Danilo Jimenez Rezende, Shakir Mohamed, and Daan Wierstra. Stochastic backpropagation and approximate inference in deep generative models. *arXiv preprint arXiv:1401.4082*, 2014.
- [25] Tim Salimans, Ian Goodfellow, Wojciech Zaremba, Vicki Cheung, Alec Radford, and Xi Chen. Improved techniques for training GANs. In *NIPS*, 2016.
- [26] Jost Tobias Springenberg. Unsupervised and semi-supervised learning with categorical generative adversarial networks. *arXiv preprint arXiv:1511.06390*, 2015.
- [27] Theano Development Team. Theano: A Python framework for fast computation of mathematical expressions. *arXiv e-prints*, abs/1605.02688, May 2016. URL <http://arxiv.org/abs/1605.02688>.
- [28] Lucas Theis, Aäron van den Oord, and Matthias Bethge. A note on the evaluation of generative models. *arXiv preprint arXiv:1511.01844*, 2015.
- [29] Ronald J Williams. Simple statistical gradient-following algorithms for connectionist reinforcement learning. *Machine learning*, 8(3-4):229–256, 1992.
- [30] Jimei Yang, Scott E Reed, Ming-Hsuan Yang, and Honglak Lee. Weakly-supervised disentangling with recurrent transformations for 3d view synthesis. In *NIPS*, 2015.

## A Detailed Theoretical Analysis

**Lemma 3.1.** *For any fixed  $C$  and  $G$ , the optimal discriminator  $D$  of the game defined by the utility function  $U(C, G, D)$  is*

$$D_{C,G}^*(x, y) = \frac{p(x, y)}{p(x, y) + p_\alpha(x, y)}, \quad (4)$$

where  $p_\alpha(x, y) := (1 - \alpha)p_g(x, y) + \alpha p_c(x, y)$  is a valid distribution.

*Proof.* Given the classifier and generator, the utility function can be rewritten as

$$\begin{aligned} U(C, G, D) &= \iint p(x, y) \log D(x, y) dy dx + (1 - \alpha) \iint p(y) p_z(z) \log(1 - D(G(z, y), y)) dy dz \\ &\quad + \alpha \iint p(x) p_c(y|x) \log(1 - D(x, y)) dy dx \\ &= \iint p(x, y) \log D(x, y) dy dx + \iint p_\alpha(x, y) \log(1 - D(x, y)) dy dx = f(D(x, y)). \end{aligned}$$

Note that the function  $f(D(x, y))$  achieves the maximum at  $\frac{p(x, y)}{p(x, y) + p_\alpha(x, y)}$ .

□

**Lemma 3.2.** *The global minimum of  $V(C, G)$  is achieved if and only if  $p(x, y) = p_\alpha(x, y)$ .*

*Proof.* Given  $D_{C,G}^*$ , we can reformulate the minimax game with value function  $U$  as:

$$V(C, G) = \iint p(x, y) \log \frac{p(x, y)}{p(x, y) + p_\alpha(x, y)} dy dx + \iint p_\alpha(x, y) \log \frac{p_\alpha(x, y)}{p(x, y) + p_\alpha(x, y)} dy dx.$$

Following the proof in GAN, the  $V(C, G)$  can be rewritten as

$$V(C, G) = -\log 4 + 2JSD(p(x, y) || p_\alpha(x, y)), \quad (5)$$

where  $JSD$  is the Jensen-Shannon divergence, which is always non-negative and the unique optimum is achieved if and only if  $p(x, y) = p_\alpha(x, y) = (1 - \alpha)p_g(x, y) + \alpha p_c(x, y)$ .  $\square$

**Corollary 3.2.1.** *Given  $p(x, y) = p_\alpha(x, y)$ , the marginal distributions are the same for  $p$ ,  $p_c$  and  $p_g$ .*

*Proof.* Remember that  $p_g(x, y) = p(y)p_g(x|y)$  and  $p_c(x, y) = p(x)p_c(y|x)$ . Take integral with respect to  $x$  on both sides of  $p(x, y) = p_\alpha(x, y)$  to get

$$\int p(x, y) dx = (1 - \alpha) \int p_g(x, y) dx + \alpha \int p_c(x, y) dx,$$

which indicates that

$$p(y) = (1 - \alpha)p(y) + \alpha p_c(y), \text{ i.e. } p_c(y) = p(y) = p_g(y).$$

Similarly, it can be shown that  $p_g(x) = p(x) = p_c(x)$  by taking integral with respect to  $y$ .  $\square$

**Theorem 3.3.** *The equilibrium of  $\tilde{U}(C, G, D)$  is achieved if and only if  $p(x, y) = p_g(x, y) = p_c(x, y)$ .*

*Proof.* According to the definition,  $\tilde{U}(C, G, D) = U(C, G, D) + \mathcal{R}_L$ , where

$$\mathcal{R}_L = E_p[-\log p_c(y|x)],$$

which can be rewritten as:

$$D_{KL}(p(x, y) || p_c(x, y)) + H_p(y|x).$$

Namely, minimizing  $\mathcal{R}_L$  is equivalent to minimizing  $D_{KL}(p(x, y) || p_c(x, y))$ , which is always non-negative and zero if and only if  $p(x, y) = p_c(x, y)$ . Besides, the previous lemmas can also be applied to  $\tilde{U}(C, G, D)$ , which indicates that  $p(x, y) = p_\alpha(x, y)$  at the global equilibrium, concluding the proof.  $\square$

**Corollary 3.3.1.** *Any additional regularization on the distances between the marginal, conditional and joint distributions of any two players, will not change the global equilibrium of  $\tilde{U}$ .*

*Proof.* This conclusion is straightforward derived by the global equilibrium point of  $\tilde{V}$ .  $\square$

**Pseudo discriminative loss** We prove the equivalence of the pseudo discriminative loss in the main text and KL-divergence  $D_{KL}(p_g(x, y) || p_c(x, y))$  as follows:

$$\begin{aligned} & D_{KL}(p_g(x, y) || p_c(x, y)) + H_{p_g}(y|x) - D_{KL}(p_g(x) || p(x)) \\ &= \iint p_g(x, y) \log \frac{p_g(x, y)}{p_c(x, y)} + p_g(x, y) \log \frac{1}{p_g(y|x)} dx dy - \int p_g(x) \log \frac{p_g(x)}{p(x)} dx \\ &= \iint p_g(x, y) \log \frac{p_g(x, y)}{p_c(x, y)p_g(y|x)} dx dy - \iint p_g(x, y) \log \frac{p_g(x)}{p(x)} dx dy \\ &= \iint p_g(x, y) \log \frac{p_g(x, y)p(x)}{p_c(x, y)p_g(y|x)p_g(x)} dx dy \\ &= E_{p_g}[-\log p_c(y|x)]. \end{aligned}$$

Note that the last equality holds as  $p_c(x) = p(x)$  and  $H_{p_g}(y|x) - D_{KL}(p_g(x) || p(x))$  is a constant with respect to  $\theta_c$ . Therefore, if we only optimize  $C$ , these two losses are equivalent.

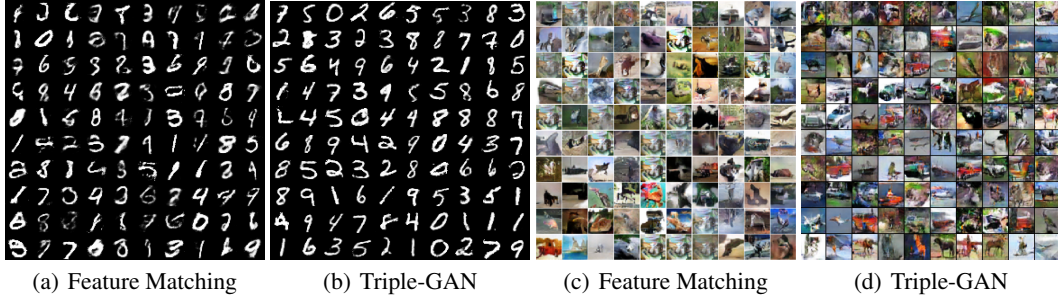


Figure 5: (a) and (c): Samples generated from Improved-GAN trained with feature matching on MNIST and CIFAR10 datasets. Strange patterns repeat on CIFAR10. (b) and (d): Samples generated from Triple-GAN.

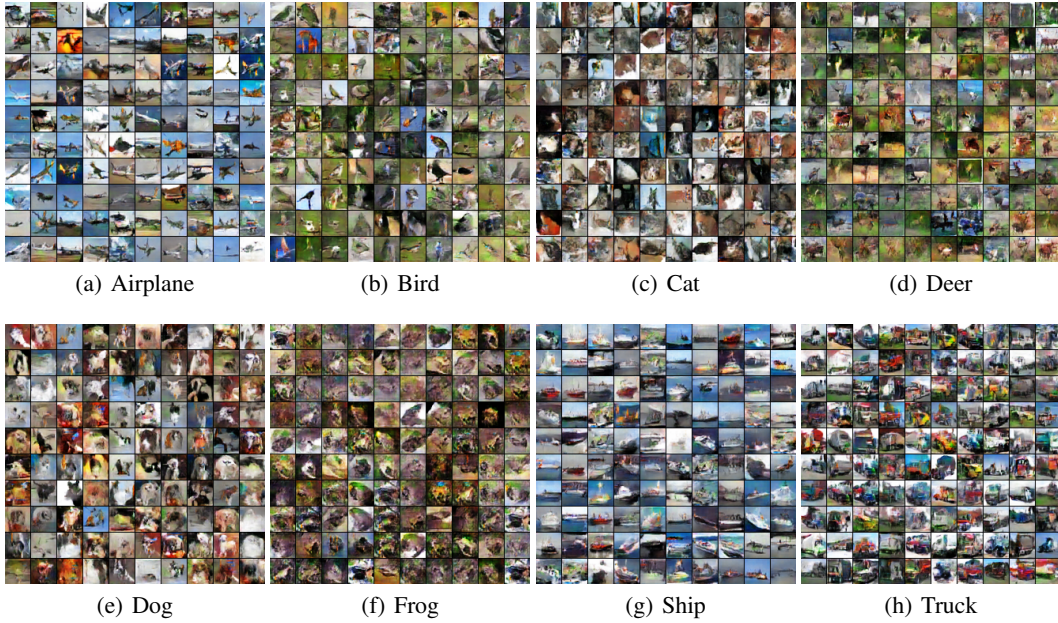


Figure 6: Samples from Triple-GAN given certain class on CIFAR10.

## B Unconditional Generation

We compare the samples generated from Triple-GAN and Improved-GAN on the MNIST and CIFAR10 datasets as in Fig. 5, where Triple-GAN shares the same architecture of generator and number of labeled data with the baseline. It can be seen that Triple-GAN outperforms the GANs that are trained with the feature matching criterion on generating indistinguishable samples.

## C Class-conditional Generation on CIFAR10

We show more class-conditional generation results on CIFAR10 in Fig. 6. Again, we can see that Triple-GAN can generate meaningful images in specific classes.

## D Disentanglement and Interpolation on the MNIST dataset

We present the disentanglement of class and style and class-conditional interpolation on the MNIST dataset as in Fig. 7. We have the same conclusion as in main text that Triple-GAN is able to transfer smoothly on the data level with clear semantics.

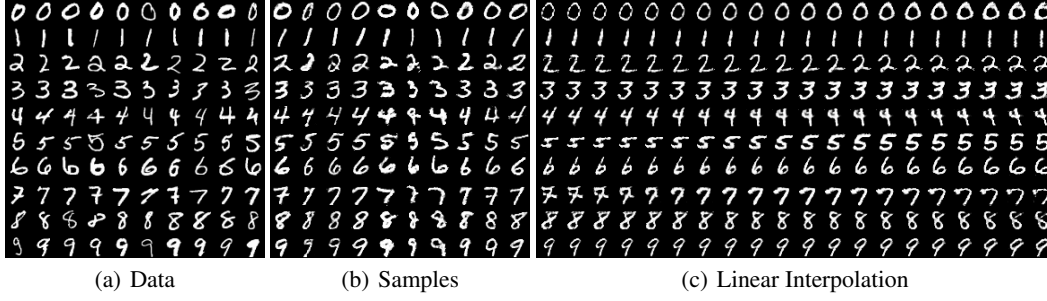


Figure 7: (a): randomly sampled MNIST data; (b) disentanglement of class and style; (c) class-conditional interpolation for Triple-GAN on MNIST.

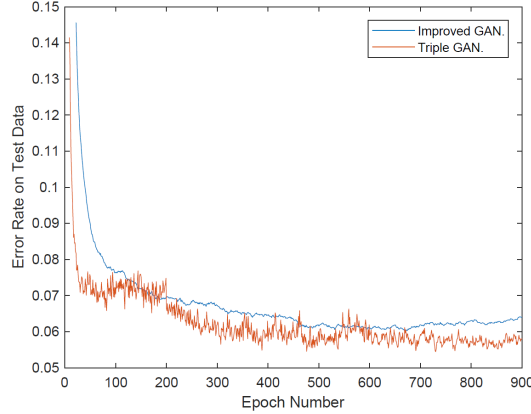


Figure 8: Convergence speed of Improved GAN and Triple-GAN on SVHN.

## E Convergence Speed

Though Triple-GAN has one more network, its convergence speed is at least comparable with Improved-GAN, as presented in Fig. 8. Both the models are trained on SVHN dataset with default settings and Triple-GAN can get good results in tens of epochs. The reason that the learning curve of Triple-GAN is oscillatory may be the larger variance of the gradients due to the presence of discrete variables. Also note that we apply pseudo discriminative loss at epoch 200 and then the test error is reduced significantly in 100 epochs.

## F Detailed Architectures

We list the detailed architectures of Triple-GAN on MNIST, SVHN and CIFAR10 datasets in Table 3, Table 4 and Table 5, respectively.

Table 3: MNIST

Classifier C	Discriminator D	Generator G
Input $28 \times 28$ Gray Image	Input $28 \times 28$ Gray Image, Ont-hot Class representation	Input Class $y$ , Noise $z$
$5 \times 5$ conv. 32 ReLU	MLP 1000 units, lReLU, gaussian noise, weight norm	MLP 500 units, softplus, batch norm
$2 \times 2$ max-pooling, 0.5 dropout	MLP 500 units, lReLU, gaussian noise, weight norm	
$3 \times 3$ conv. 64 ReLU	MLP 250 units, lReLU, gaussian noise, weight norm	
$3 \times 3$ conv. 64 ReLU	MLP 250 units, lReLU, gaussian noise, weight norm	MLP 500 units, softplus, batch norm
$2 \times 2$ max-pooling, 0.5 dropout	MLP 250 units, lReLU, gaussian noise, weight norm	
$3 \times 3$ conv. 128 ReLU	MLP 1 unit, sigmoid, gaussian noise, weight norm	
$3 \times 3$ conv. 128 ReLU		MLP 784 units, sigmoid
Global pool		
10-class Softmax		

Table 4: **SVHN**

Classifier C	Discriminator D	Generator G
Input: $32 \times 32$ Colored Image	Input: $32 \times 32$ colored image, class y	Input: Class y, Noise z
0.2 dropout $3 \times 3$ conv. 128 lReLU, batch norm $3 \times 3$ conv. 128 lReLU, batch norm $3 \times 3$ conv. 128 lReLU, batch norm $2 \times 2$ max-pooling, 0.5 dropout	0.2 dropout $3 \times 3$ conv. 32, lReLU, weight norm $3 \times 3$ conv. 32, lReLU, weight norm, stride 2 0.2 dropout	MP 8192 units, ReLU, batch norm Reshape $512 \times 4 \times 4$ $5 \times 5$ deconv. 256. stride 2, ReLU, batch norm
$3 \times 3$ conv. 256 lReLU, batch norm $3 \times 3$ conv. 256 lReLU, batch norm $3 \times 3$ conv. 256 lReLU, batch norm $2 \times 2$ max-pooling, 0.5 dropout	$3 \times 3$ conv. 64, lReLU, weight norm $3 \times 3$ conv. 64, lReLU, weight norm, stride 2 0.2 dropout	$5 \times 5$ deconv. 128. stride 2, ReLU, batch norm
$3 \times 3$ conv. 512 lReLU, batch norm NIN, 256 lReLU, batch norm NIN, 128 lReLU, batch norm Global pool 10-class Softmax, batch norm	$3 \times 3$ conv. 128, lReLU, weight norm $3 \times 3$ conv. 128, lReLU, weight norm Global pool MLP 1 unit, sigmoid	$5 \times 5$ deconv. 3. stride 2, sigmoid, weight norm

Table 5: **CIFAR10**

Classifier C	Discriminator D	Generator G
Input: $32 \times 32$ Colored Image	Input: $32 \times 32$ colored image, class y	Input: Class y, Noise z
Gaussian noise $3 \times 3$ conv. 128 lReLU, weight norm $3 \times 3$ conv. 128 lReLU, weight norm $3 \times 3$ conv. 128 lReLU, weight norm $2 \times 2$ max-pooling, 0.5 dropout	0.2 dropout $3 \times 3$ conv. 32, lReLU, weight norm $3 \times 3$ conv. 32, lReLU, weight norm, stride 2 0.2 dropout	MLP 8192 units, ReLU, batch norm Reshape $512 \times 4 \times 4$ $5 \times 5$ deconv. 256. stride 2 ReLU, batch norm
$3 \times 3$ conv. 256 lReLU, weight norm $3 \times 3$ conv. 256 lReLU, weight norm $3 \times 3$ conv. 256 lReLU, weight norm $2 \times 2$ max-pooling, 0.5 dropout	$3 \times 3$ conv. 64, lReLU, weight norm $3 \times 3$ conv. 64, lReLU, weight norm, stride 2 0.2 dropout	$5 \times 5$ deconv. 128. stride 2 ReLU, batch norm
$3 \times 3$ conv. 512 lReLU, weight norm NIN, 256 lReLU, weight norm NIN, 128 lReLU, weight norm Global pool 10-class Softmax with weight norm	$3 \times 3$ conv. 128 lReLU, weight norm $3 \times 3$ conv. 128, lReLU, weight norm Global pool MLP 1 unit, sigmoid, weight norm	$5 \times 5$ deconv. 3. stride 2 tanh, weight norm